

## Protein Adsorption onto Hydroxyapatite/Chondroitin Sulfate Microparticles

Hajime Watanabe\*\*\*, Toshiyuki Ikoma\*\*, Guoping Chen\*\*\* and Junzo Tanaka\*\*\*\*\*

\* Graduate School of Pure and Applied Sciences University of Tsukuba,  
Tenodai 1-1-1 Tsukuba, Ibaraki 305-8571, Japan

Fax: 81- 029-860-4714, e-mail: WATANABE.Hajime@nims.go.jp, Guoping.Chen@nims.go.jp

\*\* Biomaterials Center, National Institute for Materials Science, Namiki 1-1, Tsukuba, Ibaraki 305-0044, Japan

Fax: 81-29-851-8291, e-mail: IKOMA.Toshiyuki@nims.go.jp

\*\*\* Department of Metallurgy and Ceramics Science, Tokyo Institute of Technology,  
Ookayama 2-12-1, Meguro, Tokyo 152-8550, Japan  
e-mail: Junzo.Tanaka@ceram.titech.ac.jp

Microparticles of hydroxyapatite (HAp) and chondroitin sulfate (ChS) composites were fabricated by a spray-dry method. The elution of ChS from the microparticles with different contents of ChS and molecular weights was analyzed by soaking into phosphate buffer saline (PBS), 10% PBS and distilled water; the increase of the ChS contents and the concentration of phosphate ions increased the ChS elution of which rate was decreased with larger molecular weight of ChS. The protein adsorptions of cytochrome c (cytc) and bovine serum albumin (BSA) on the microparticles were analyzed; the adsorption amount of cytc was increased with the ChS contents and its molecular weight, and that of BSA was apparently decreased with the contents of ChS. The increase of phosphate concentrations in buffers decreased the amount of protein adsorptions.

Key words: Hydroxyapatite, Chondroitin Sulfate, Microparticle, Elution, Adsorption, Protein, Molecular Weight

### 1. INTRODUCTION

Hydroxyapatite ( $\text{Ca}_{10}(\text{PO}_4)_6(\text{OH})_2$ ; HAp) shows a high biocompatibility with no inflammatory reaction and osteoconductivity. Thus, HAp has been widely used for a bone substitute material [1-3]. The moderate adsorption property of proteins onto HAp increases uses for filler of chromatography and drug delivery carriers. Recently, HAp nanocrystals or microparticles are applied for the sustained release of cytochrome c (cytc), interferon and other protein drugs, which suggests that the HAp has a potential for a controlled release carrier [4, 5]. HAp porous ceramics loaded with therapeutic agents have been also developed for the delivery system and the time controlled release carrier [6].

Chondroitin sulfate (ChS), one of the most abundant glycosaminoglycans in human body, strongly interacts with HAp and plays an important role for the modulators of mineralization, cell differentiation and proliferation [7]. Negatively charged groups on ChS, such as carboxyl and sulfate groups, are nucleation site of HAp (mineralization), and can attract the amino groups of basic proteins and consequently form ion complexes of proteins. The cytokines, such as bFGF, TGF- $\beta$  and BMP etc., are basic proteins which promote the mineralization *in vivo*. The spherical porous microparticles of HAp/ChS nano-composites have both the properties and show higher protein adsorption ability and bonding affinity than that of HAp [8, 9].

In the present study, the spherical porous microparticles of HAp/ChS nanocomposites were fabricated by a wet method and a subsequent spray dry method. The spray drying method has a benefit for a large amount of the production of the porous HAp particles with high specific surface area at once in the industrial

process. The different molecular weight of ChS was employed for the elucidation of protein adsorption ability and elution of ChS from the microparticles. The maximum adsorption amount and binding affinity of cytochrome c (cytc) and bovine serum albumin (BSA) for the microparticles were discussed.

### 2. MATERIALS AND METHODS

#### 2.1 Materials

Pure  $\text{CaCO}_3$  powder was heated at 1050°C for 3 hours, and the resultant CaO powder was hydrated with distilled water to produce  $\text{Ca}(\text{OH})_2$ . 1000ml of 0.15 mol/l  $\text{H}_3\text{PO}_4$  solution was slowly dropped into 1000ml of 0.25 mol/l  $\text{Ca}(\text{OH})_2$  suspension without or with sodium ChS (Seikagaku Co. Tokyo, Japan; the MW of 15, 20 and 35 KDa with the 6-ChS/4-ChS ratio of 2/1) at room temperature. The theoretical weight ratios of ChS/HAp were 2.0 and 5.0wt%, respectively. The suspensions obtained were aged for 12 hours; the final pH was adjusted to approximately 8.0 [10].

The HAp/ChS microparticles were fabricated by mini spray dryer (Büchi, B-290): the suspensions were atomized under a pressure of 0.56 MPa at a flow rate of 5.0 ml/min, and a gas flow was adjusted to 30m<sup>3</sup>/h with inlet and outlet temperatures 180 and 70 °C.

#### 2.2 Characterization

The morphology of the microparticles obtained was observed by scanning electron microscopy (SEM) with the acceleration voltage of 20kV after coating with the platinum. The specific surface areas and total pore volumes were determined by Brunauer-Emmett-Teller (BET) method with nitrogen gas. The particle size distributions in distilled water were analyzed by laser

diffraction particle size analyzer.

The content of ChS in the microparticles was measured by a phenol-sulfuric acid method at the wave length of 490nm; 50mg of the microparticles were dissolved in 10ml of hydrochloric acid solution (0.1mol/l).

### 2.3 Elution of ChS from the microparticles

The elution rates of ChS from the microparticles in distilled water (DW), 10% diluted PBS and PBS were analyzed; 50mg of the microparticles were dispersed in 10ml of the solutions for 1 hour at 21.5°C. The suspension was filtered to remove the microparticles and the supernatant was measured by the phenol-sulfuric acid method.

### 2.4 Protein adsorption tests

The protein adsorption properties of the microparticles were analyzed by using cytc (MW=12KDa, pI=10.2) and BSA (MW=66KDa, pI=4.8). The cytc has 104 amino acid residues with basic amino acids [11]. On the other hand, BSA is the representative acidic protein, and has been generally used as a model protein. The cytc and BSA were purchased from the Wako Chemical Co..

The time dependences of the cytc adsorption amounts in 10% diluted PBS were analyzed at 21.5 °C; 20mg of the microparticles with different contents of ChS (MW=15kD) was dispersed in 6ml of the solution with 2.0mg/ml for 10 to 720 min.

The concentration dependences of the cytc and BSA in DW, 10% diluted PBS and PBS were analyzed at 21.5 °C; 20mg of the microparticles with different MW and content of ChS was dispersed in 6ml of the solutions with different protein concentrations at 0 to 2.0mg/ml for 4 hours.

The pH dependences of the protein adsorption were analyzed in the phosphate buffers at pH of 5.5, 7.3 and 8.0 mixing Na<sub>2</sub>HPO<sub>4</sub> (10mM) with NaH<sub>2</sub>PO<sub>4</sub> (10mM) solutions; 20mg of the microparticles with 2.0% of ChS (MW = 15kD) were dispersed in the buffer solutions with 2.0mg/ml of the protein concentration.

All the specimens were centrifuged for 10 minutes, and the supernatants were analyzed by visual ultraviolet spectroscopy (vis-UV) at 520 nm for cytc, and at 276nm for BSA.

### 2.5 Maximum amount and bonding affinity

The adsorption isotherm curve of proteins is obtained from the experimental data, which is independent on any adsorption models [11]. The plot of the adsorption amount versus equilibrium concentration of proteins

gives the maximum amount and bonding affinity. Most of the protein adsorption can fit well to the Langmuir-type model as follows.



Where P = protein in solution, A = unoccupied surface site and PA = occupied surface site, Langmuir-type adsorption gives

$$K[P][A_T] - K[P][AP] = [PA] \quad (2)$$

Linearization of Eq. (2) gives

$$[P]/[PA] = 1/K[A_T] + [P]/[A_T] \quad (3)$$

Where [A<sub>T</sub>] is the maximum number of adsorption sites per unit of surface area of the protein (mg/m<sup>2</sup>) and K reflects the affinity that the protein molecules bonded on the adsorption sites. The experimental data should satisfy the linearization followed by the Eq. (2). According to Eq. (3), a plot of 1/[PA] against 1/[P] should yield a straight line from which K and A<sub>T</sub> can be determined from the slope and intercept of the straight line.

## 3. RESULT AND DISCUSSION

### 3.1 Characterization

The ChS contents were almost the same as the starting compositions, which depend on the yield of the HAp precipitated. The particle size distribution was 1.0 to 10μm measured by the laser diffraction method and the mean particle size was approximately 4μm for all the samples.

Fig. 1 shows the SEM image of the typical microparticle including 1.7wt% of ChS (MW:15KDa). The microparticles obtained had the perfectly spherical shape and the surface structure is smooth compared with pure HAp microparticle. The precipitations of HAp/ChS nanocomposites had the ordered nanostructure [8]: the *c*-axis of HAp nanocrystals was oriented along the ChS molecular. The ChS was homogeneously distributed in the microparticles. The increase of ChS content caused the smoother surface from the observations of FE-SEM (data not shown here). The particle size distribution was almost matched to the laser diffraction analyses.

### 3.2 Elution of ChS from the microparticles

Table. I shows the specific surface areas and the porosities of the microparticles obtained. The porosities were calculated from the total pore volume and the theoretical density (3.16g/cm<sup>3</sup>) of HAp. The increase of the content of ChS with all the MWs except for 35KDa increased the specific surface areas and decreased a slight amount of the porosities.

Table. I Physico-chemical properties of HAp/ChS microparticles with different MW of ChS.

ChS wt%	MW	Specific surface area (m <sup>2</sup> /g)	Total pore volume (ml/g)	Porosity (%)
0(HAp)	-	102.5	0.744	70.2
1.7±0.4	15KDa	108.7	0.754	70.5
4.0±0.4	15KDa	116.0	0.687	68.5
1.9±0.1	20KDa	109.8	0.706	69.1
4.3±0.3	20KDa	116.5	0.623	66.5
1.8±0.1	35KDa	112.0	0.713	69.3
4.8±0.1	35KDa	107.3	0.659	67.6

ChS wt%: Mean value ± SD (n = 4 for each sample).

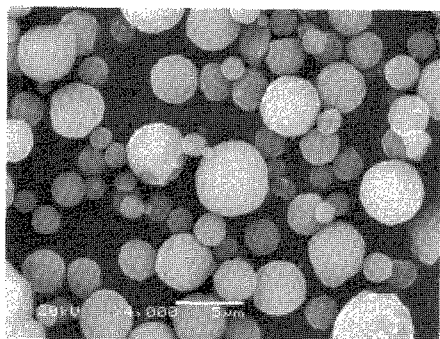


Fig. 1 A SEM image of HAp/ChS1.7wt% (MW:15KDa) microparticles obtained.

Fig. 2 shows the result of the ChS elution from the microparticles in DW, 10% diluted PBS and PBS. The elution rates of ChS increased with the increase of the phosphate concentrations. The elution rates of ChS tended to decrease with the increase of the MWs of ChS in the microparticles. These results indicated that the bonding number of carboxyl and/or sulfate groups to the C site of HAp (calcium site) was the dominating factor in the elution process. The bonding number relates to the MW of ChS. The reduction of the binding number of ChS molecules to HAp surfaces may be attributed to the aggregates of ChS in solution due to the high MW of ChS [12]. In this study, however, the ChS molecule bonded to HAp crystals without aggregating of the ChS through the synthesis of the HAp/ChS nanocomposites. Thus, the binding affinity between ChS molecules and HAp crystals is increased due to the increase of the number of bondings.

3. 3 Protein adsorption tests

Fig. 3 shows the time dependence for the adsorption of cytc onto the HAp/ChS microparticles with 1.7 and 4.0wt% of ChS (15KDa) in 10% diluted PBS. The maximum adsorption was attained at 240min for HAp and 360min for HAp/ChS microparticles with 1.7wt% of ChS, but not with 4.0wt% in 720min. The maximum adsorption amount apparently increased with the increase of ChS contents. In the following adsorption

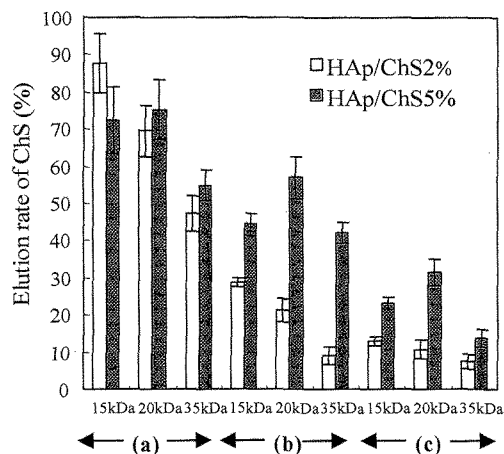


Fig. 2 The elution rates of ChS from HAp/ChS microparticles at different ChS contents and MWs of ChS in (a) PBS, (b) 10% diluted PBS and (c) D.W. (n = 4).

experiments, the time period of 4h was employed for the adsorption experiments.

The adsorption isotherms to the microparticles in D.W. and 10% diluted PBS with different concentration of cytc were followed to the Langmuir's equation regardless of the change of ChS contents, while those in PBS were not followed. The maximum adsorption amounts of cytc onto the HAp, the HAp/ChS microparticles with 1.7 and 4.0 wt% of ChS (MW: 15KDa) in D.W. were 1.06, 1.94 and 2.41mg/m<sup>2</sup>, and the affinity constants were 8.44, 23.6 and 10.4, respectively. On the other hand, those on HAp in PBS were almost the same as on HAp/ChS with any wt% of ChS.

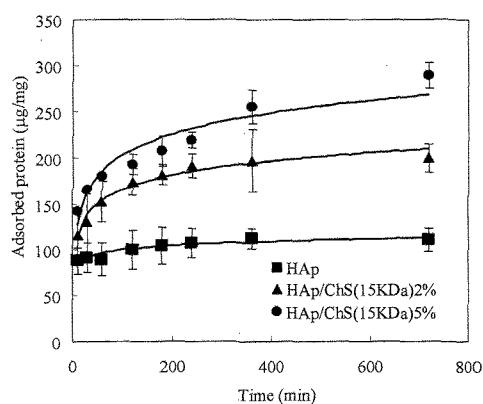


Fig. 3 Time profiles for the adsorption of cytc onto HAp and HAp/ChS(MW:15KDa) microparticles in 10% diluted PBS (n = 4).

Fig. 4 shows the results of the maximum adsorption amounts of cytc and the affinity constants with cytc in 10% diluted PBS. The adsorption isotherms of cytc onto the HAp/ChS microparticles with any MWs of ChS in 10% diluted PBS were followed to the Langmuir's equation. For the microparticles with 2.0wt% of ChS, the increase of the MW of ChS caused the increase of the affinity constants and the slight decrease of the maximum adsorption amount. While, for the microparticles with 5.0wt% of ChS, the affinity constant was independent of the MW, however the maximum adsorption amount of cytc increased with the increase of the MW.

The pH dependence of the adsorption amount and affinity constants of cytc for the microparticle with 1.7wt% of ChS (15kDa) were measured; the pH of the phosphate buffers was changed to 6.2, 7.3 and 7.8 from 5.5, 7.3 and 8.0 of initial pH values, respectively. The affinity constants were 30.1, 12.4 and 12.0 at each pH and the maximum adsorption amounts were 1.7, 2.1 and 2.5 mg/m<sup>2</sup>. On the other hand, for the microparticle with 4.0wt% of ChS (15KDa), the affinity constants at pH of 6.2 and the maximum amount of cytc adsorbed was 2.5 mg/m<sup>2</sup>. At the final pH values of 7.30 and 7.80, the adsorption isotherms were not followed to the Langmuir's equation.

Fig. 5 shows the adsorption isotherms of BSA onto HAp or HAp/ChS microparticles with 15, 20 and 35KDa of MW in 10% diluted PBS. The adsorption isotherms were followed to the Langmuir's equation regardless of the change of ChS content. The maximum adsorption

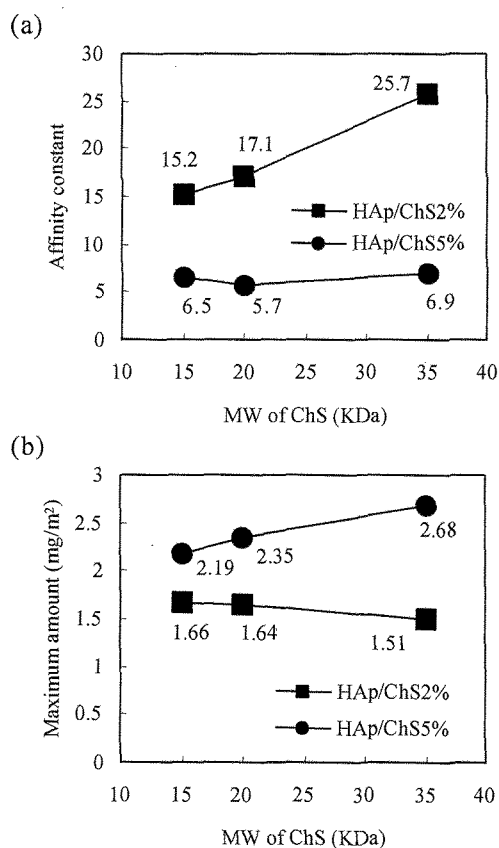


Fig. 4 Effect of MW of ChS onto (a) affinity constant and (b) maximum amount of cytc adsorbed in 10% diluted PBS

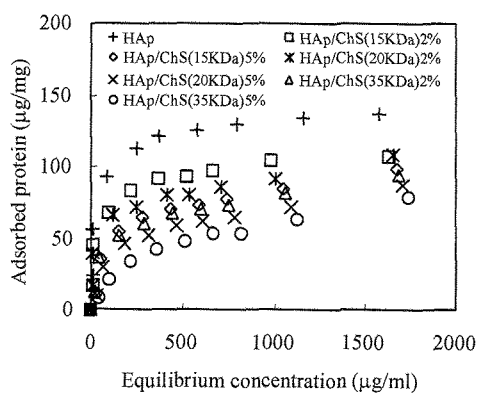


Fig. 5 Adsorption isotherms for BSA onto HAp and HAp/ChS(15, 20 and 35KDa) microparticles in 10% diluted PBS.

amount of BSA onto HAp microparticles was 1.36mg/m<sup>2</sup>. In relation to the microparticles with 2.0wt% of ChS, those of the microparticles with 15, 20 and 35KDa of the MWs of ChS were 1.02, 0.96 and 0.77mg/m<sup>2</sup>, respectively. While in relation to the microparticles with 5.0wt% of ChS, those were 0.78, 0.70 and 0.68mg/m<sup>2</sup> for 15, 20 and 35KDa, respectively. The affinity constant of the HAp microparticles was 22.9. Those of the microparticles with 2.0wt% of ChS were 15.5, 9.6 and 9.2 and those of the microparticles

with 5.0wt% of ChS were 9.2, 7.0 and 3.8 for 15, 20 and 35KDa, respectively. Both the maximum amount and the affinity constant about the HAp microparticles showed the highest value in 10% PBS. These indicated that the adsorption was inhibited by the electrostatic repulsion between the ChS molecules in the microparticles and the BSA molecules in the solution. Both the maximum amount and the affinity constant were decreased with the increase of MW of ChS in the microparticles. In PBS, the maximum amounts of BSA onto the HAp and HAp/ChS2.0 and 5.0wt% with 15KDa of the MW were 0.71, 0.60 and 0.63mg/m<sup>2</sup>, respectively. Their affinity constants of the HAp and HAp/ChS2.0 and 5.0wt% with 15KDa of the MW were 5.1, 3.1 and 3.2, respectively.

#### 4. SUMMARY

The HAp/ChS microparticles were fabricated by a spray dry method. The elution rates of ChS from the microparticles decreased with the increase of the MW of ChS and the phosphate concentrations. The affinity constant and the maximum amount of cytc adsorbed were increased with the increase of the MW and the decrease of the phosphate concentration. On the other hand, the affinity constant and the maximum amount of BSA were decreased with the increase of the MW and the phosphate concentration.

#### 5. REFERENCES

- [1] R. Rossa, *J. Oral Implantol*, 17, 184-92 (1991).
- [2] L. G. Ellies, J. M. Carter, J. R. Natiella, J. D. B. Featherstone, D. G. A. Nelson, *J. Biomed. Mater. Res.*, 22, 137-148 (1988).
- [3] G. L. Delange, C. Deputter, F. L. J. A. Dewijs, *J. Biomed. Mater. Res.*, 24, 829-845 (1990).
- [4] Y. Mizushima, T. Ikoma, J. Tanaka, K. Hoshi, T. Ishiikawa, Y. Ogawa, A. Ueno, *J. Controlled Release*, 110, 260-265 (2006).
- [5] T. Matsumoto, M. Okazaki, M. Inoue, S. Yamaguchi, T. Kusunose, T. Toyonaga, Y. Hamada, J. Takahashi, *Biomaterials*, 25, 3807-3812 (2004).
- [6] M. Itokazu, T. Sugiyama, T. Ohno, E. Wada, Y. Katagiri, *J. Biomed. Mater. Res.*, 39, 536 (1998).
- [7] G. K. Hunter, S. K. Azigety, *Matrix*, 12, 362 (1992).
- [8] T. Ikoma, N. Azuma, S. Itoh, H. Omi, S. Nishikawa, S. Toh J. Tanaka, *Key Eng. Mater.*, 288-289, 159-162 (2005).
- [9] H. Watanabe, T. Ikoma, G. Chen, A. Monkawa, J. Tanaka, *Key Eng. Mater.*, 309-311, 533-536 (2006).
- [10] R. E. Dickerson, T. Takano, D. Eisenberg, O. B. Kallai, L. Samson, A. Cooper, E. Margoliash, *J. Biol. Chem.*, 246, 1511 (1971).
- [11] E. C. Moreno, M. Kresak, D. I. Hay, *Calcif. Tissue Int.*, 36, 48-59 (1984).
- [12] S. G. Rees, D. T. H. Wassell, G. Embery, *Biomaterials*, 23, 481-489 (2002).

(Received January 15, 2006; Accepted March 30, 2006)